Bulletin of the Earthquake
Research Institute
Vol. 46 (1968), pp. 1103-1125

53. *Source Locations of Elastic Shocks in the Fracturing Process in Rocks (1).*

By Kiyoo Mogi,

Earthquake Research Institute.

(Read May 28, 1968.—Received July 31, 1968.)

Abstract

Source locations of elastic shocks caused by micro-fractures in various rocks subjected to bending stress were determined by a new experimental system, which consists of piezo-electric type transducers, amplifiers, dual-beam synchroscopes and moving cameras. In heterogeneous rocks, elastic shocks markedly increase before a main rupture. In the earlier stage, sources of elastic shocks locate at random in a rock sample. In the later stage, they concentrate in one or more limited regions in the sample, and the shock activity in other regions decreases. Just before rupture, one of the highly active regions extends in the direction perpendicular to the applied tensile stress. In rocks with homogeneous structure, however, rupture takes place suddenly without the above-mentioned micro-fracturing process. These results observed in laboratory are very helpful to understand the process of foreshock occurrence in earthquakes.

1. Introduction

In previous papers (Mogi, 1962a, 1962b, 1962c, 1963a, 1963b, 1967b), we have systematically studied micro-fracturing behaviors of various rocks and other heterogeneous brittle materials subjected to external stresses, by observing elastic waves of shock type accompanying micro-fractures. We called these elastic waves of shock type caused by fractures *elastic shocks*. One of the purposes of the previous studies of elastic shocks was to clarify the mechanical process of rock failure. Another purpose of the studies was to get a clue to understand the earthquake generation mechanism, from the standpoint of the fracture theory of earthquakes in which earthquakes are thought to be caused by brittle fracturing of the earth's surface layer. These laboratory studies of elastic shocks have led to the physical understanding of some

important features of earthquakes. The present study is a continuation of these previous studies.

Our previous studies (e.g. Mogi, 1962a) and studies by other workers (Obert and Duvall, 1942; Vinogradov, 1962; Watanabe, 1963; Suzuki and Hamaguchi, 1966; Nagumo and Hoshino, 1968; Scholz, 1968a) have been mainly devoted to the time and the magnitude distributions of elastic shocks in the fracturing process. However, systematic studies of other interesting features, such as radiation patterns and source locations of elastic shocks, have been left undone up to now. New experimental devices used in the present study have made it possible to investigate these features of elastic shocks. In this paper, source locations of elastic shocks in the fracturing process in various rocks subjected to a bending stress are discussed.

Recently, Scholz (1968b) tried to determine source locations of elastic shocks prior to rupture of a granite specimen, by use of initial motions of S-waves. He remarked a clustering of micro-fracturing on the eventual fault plane. In his study, however, a total of twenty-two shocks only were located and results were accompanied by appreciable errors, so that detailed features in source locations in the fracturing process were not clear.

The present experimental procedure by use of initial motions of P-waves is very simple and provides accurate results. By this new technique, a large number of source locations in successive stages in fracturing process have been determined for various rock specimens with different structures.

Source locations observed in the present experiment help us to understand the process of fracture propagation prior to rupture, and also the process of foreshock occurrence in earthquakes.

2. Experimental procedure

2-1. New technique for measurement of elastic shocks

A failure of a rock sample is preceded by anomalous increase of deformation and usually by the occurrence of elastic shocks caused by micro-fracturing. According to a previous study (Mogi, 1962a), the process of occurrence of elastic shocks is characterized as a stochastic process, so that the occurrence of each shock cannot be predicted. These elastic shocks are very high frequency elastic waves, although they contain also a low frequency part. The predominant period of an elastic

shock accompanying micro-fracturing of 3 millimeter length may be roughly estimated 1 μ sec from (velocity of crack propagation) $\times$ (crack length). Scholz (1968b) pointed out such very high frequency waves in elastic shocks. In general, amplitudes of elastic shocks vary widely.

In previous studies except for Scholz's ones, elastic shocks were recorded by an electromagnetic oscillograph after high amplification of signals from piezo-electric type transducers. The system was suitably applied to investigations of some features, such as the magnitude-frequency relation and the time distributions of elastic shocks. However, the frequency range in the system is too low to observe wave forms of elastic shocks and to detect differences in arrival times of elastic shocks within small rock samples.

The synchroscope-moving camera system used in the present study makes it possible to observe such very high frequency waves and to detect a small time difference, such as 1 μ sec. The present experimental arrangement is schematically shown in Fig. 1. The transducers used in

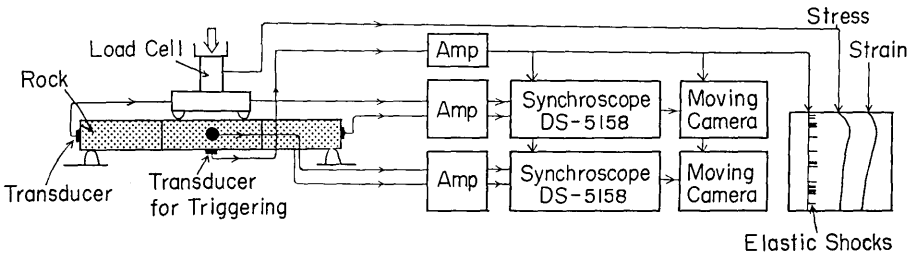

Fig. 1. Experimental system for measurement of elastic shocks caused by micro-fracturing.

the present study are lead-titanate-zirconate compressional mode disks, 10 mm in diameter and 3 mm thick. To observe completely an initial part of a signal, transducers for triggering of synchroscopes and cameras were situated close to a source region, and transducers for observation of signals were placed at a distance from the source region. Amplification was achieved by pre- and main-amplifiers of which frequency response was flat from 10 kz to 1 Mhz. Signals traced in two Iwasaki DS-5158 dual beam synchroscopes were photographed by Borex H16M moving cameras which had been ready for a shot. Just after photographing, a single frame of a film was moved and the cameras were ready for the next shot. Two traces were recorded in a single frame and one micro-second difference in arrival time between two traces was detect-

able. For time recording, a watch was photographed on the same film and the time in seconds can be read from it. The applied load and the deformation of samples were measured by meters of electric-resistance strain gage type and they were continuously recorded together with pulses showing the occurrence of elastic shocks.

This system is very suitable for our present purpose in the following respects:

(1) Almost all shocks, which are larger than a fixed magnitude, can be observed for short or long time experiments.

(2) A micro-second time difference between two traces is detectable, so that source locations of elastic shocks in a small sample can be determined accurately.

(3) By suitable setting of transducers for triggering synchroscopes, the wave shape of elastic shocks including an initial motion can be observed.

(4) Multi-trace observations are possible by increase of channels in the same system.

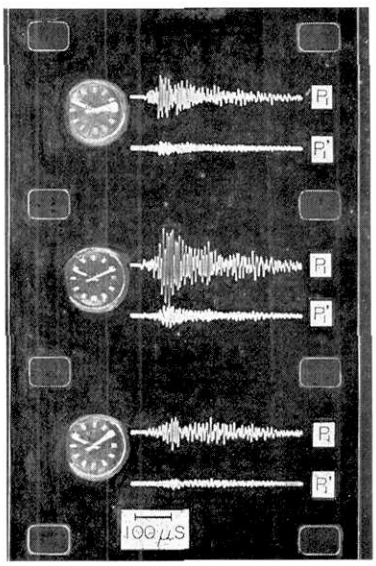

(a) Each frame shows two traces from the same transducer by different magnifications.

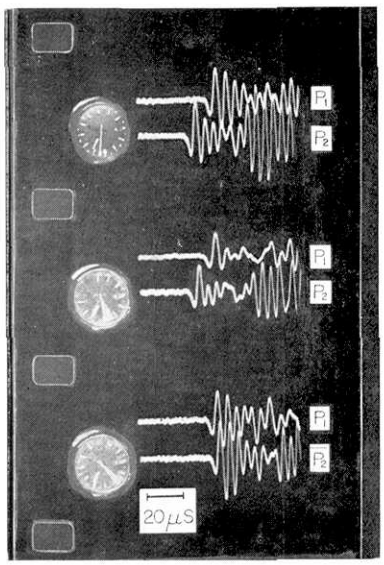

(b) Each frame shows two traces from different transducers P_1 and P_2 in Fig. 3.

Fig. 2. Examples of records of elastic shocks observed in bending experiment of a granite specimen. Arrival times in seconds are indicated by the watch photographed in each frame.

Some examples of observed signals are represented in Figs. 2(a) and (b). The two traces in each single frame in Fig. 2(a) are records of the same signals with different magnifications. Such observations with different magnifications have been made for discussions of magnitudes of elastic shocks with very different magnitudes. Two traces in each frame in Fig. 2(b) show records of the same shocks from different transducers situated at different places. From differences of arrival time of P-waves between two traces, locations of sources are determined in millimeters in many cases. Furthermore, by this experimental technique, radiation patterns of elastic waves, frequency spectrum and other features can also be investigated.

2-2. Determination of source locations of elastic shocks

In the present study, a bending stress has been applied to rock samples. Initially the stress was applied with a relatively high rate and then the stress rate gradually was decreased. Before rupture, the stress was held at a nearly constant value. This mode of loading is suitable for studying the fracturing process prior to rupture.

The sample shape and the loading system are shown in Figs. 3 and 4. By this application of a uniform moment to the central part of the sample, the upper and the lower sides are stressed in compression and tension, respectively. Since the tensile strength of brittle rocks at atmospheric pressure is about one-tenth of the compressional one, fractures take place only on the tensile side in the central part, particularly in the surface layer. Thus, if the stress gradient in depths is ignored, this experiment is essentially equivalent to a simple tension test, in which the tensile stress on the surface layer is uniform in the central part of the sample. Observations in combined stress systems will be made in the next studies.

(a) *One dimensional case*

At first, one dimensional locations of sources of elastic shocks in a direction of tensile stress ($\overline{OL}$) have been observed. Locations of transducers are shown in Fig. 3. P_1 and P_2 are transducers for measurement of signals and P_t is a transducer for triggering a synchroscope-camera system. A delay of arrival times of shocks at P_1 and P_2 from P_t makes it possible to observe initial motions of elastic shocks. Examples of signals observed at P_1 and P_2 in the fracturing process in a granite sample are shown in Fig. 2(b). Since the velocity of P-waves is known,

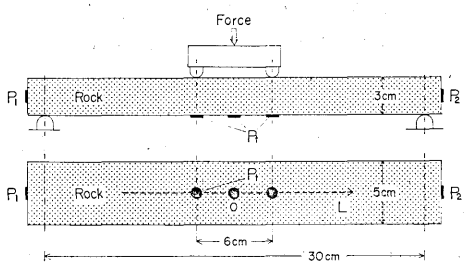

Fig. 3. The sample and transducers used in studying one-dimensional source locations of elastic shocks in rocks subjected to bending stress. P_1 and P_2: transducers for shock observation; P_t: transducers for triggering synchroscopes and cameras.

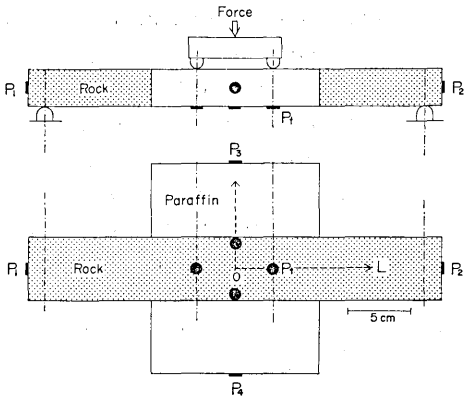

Fig. 4. The sample and transducers used in studying two-dimensional source locations of elastic shocks. P_1 and P_2: transducers for shock observation; P_t: transducers for triggering synchroscopes and cameras.

locations of sources in the $\overline{OL}$ direction can be determined from the difference in arrival time of P-waves between two traces.

(b) *Two dimensional case*

Two dimensional locations of sources can be determined by applying the above-mentioned method to two directions. Test specimens used in the present study are shown in Fig. 4. Measurements for the $\overline{OL}$ direction are similar to that in the one dimensional case. Locations in the direction to perpendicular to $\overline{OL}$ are measured from the difference in arrival times between P_3 and P_4. Strictly speaking, two dimensional locations of sources of elastic shocks can be calculated from these two differences in arrival times in consideration of velocity distribution. To obtain a delay time at P_3 and P_4, paraffin blocks were stuck on both sides of the rock sample. For the visco-elastic properties of paraffin, the paraffin blocks do not affect seriously the stress distribution, but they act as good mediums for propagation of elastic shocks. Similarly, three dimensional source locations can be determined by applying the method to three directions.

2-3. Materials used

Three granites, an andesite, a trachyte and three marbles were used in the bending experiment. Their mechanical properties and petrographic

features are described in previous papers: Inada granite, Shirochōba andesite, Mizuho trachyte, Yamaguchi fine-grained and coarse-grained marbles (Mogi, 1964); Mannari granite (Mogi, 1965); Kitagi granite (Mogi, 1962a). Mechanical structures of the granites, the andesite and the coarse grained marble are considerably heterogeneous and those of the trachyte and the fine-grained marble are nearly homogeneous. Measurements were made on four or five specimens for each rock. Compression tests were done on Saku-ishi tuff (Mogi, 1965) which is porous and non-uniform in structure.

3. Experimental results

As seen in Figs. 2(a) and (b), observed elastic shocks are quite similar to earthquake waves in shape. In some cases, the S-phase cleary can be identified, but in many cases the phase is not clear. The predominant periods of initial parts of elastic shocks observed at P_1 and P_2 were in the range from 5 μs to 10 μs, but this range may not indicate periods at sources, because of marked attenuation of high frequency waves in rock samples.

The processes of the increase of elastic shocks prior to rock failure were ascertained by the present experiment. The results agree with the previous conclusion (e.g. Mogi, 1962a) that the elastic shock activity is higher in more heterogeneous rocks. This feature will be discussed again below, in consideration with source locations of elastic shocks.

As an example of the pattern of increase of elastic shock activity, the frequency curve and the axial and lateral strain curves in a Saku-ishi tuff sample subjected to uniaxial compression are shown in Fig. 5. In this compression test, a new sample shape reported in a previous paper (Mogi, 1966) was used to eliminate stress concentration at the end of rock sample. As discussed by Scholz (1968a), the accumulated frequency of elastic shocks and the non-linear part of the volumetric strain $(\Delta V/V)_{ne}$ increase in parallel before rupture. This is consistent with the fact that elastic shocks occur due to micro-fracturing in rock.

3-1. One-dimensional source locations of elastic shocks

a) *Yamaguchi marbles with different grain sizes*

Three marbles with different grain sizes have been studied. Their

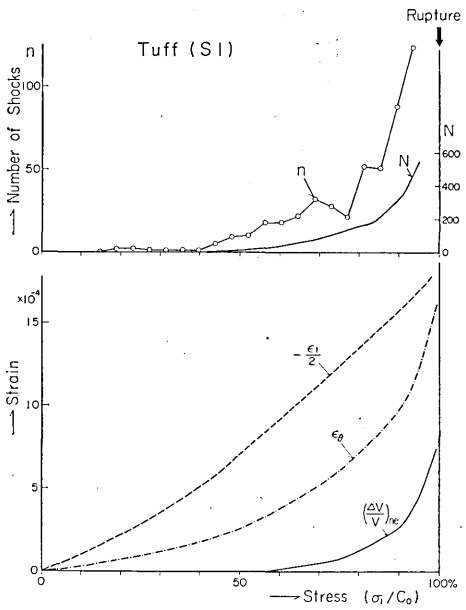

Fig. 5. Frequencies of elastic shocks (above) and strains (below) as functions of applied stress, in a uniaxial compression test of Sakuishi tuff. n and N: frequency and accumulated frequency of elastic shocks; ϵ_1 and ϵ_θ: axial and lateral strains; $(\Delta V/V)_{ne}$: non-elastic volumetric strain.

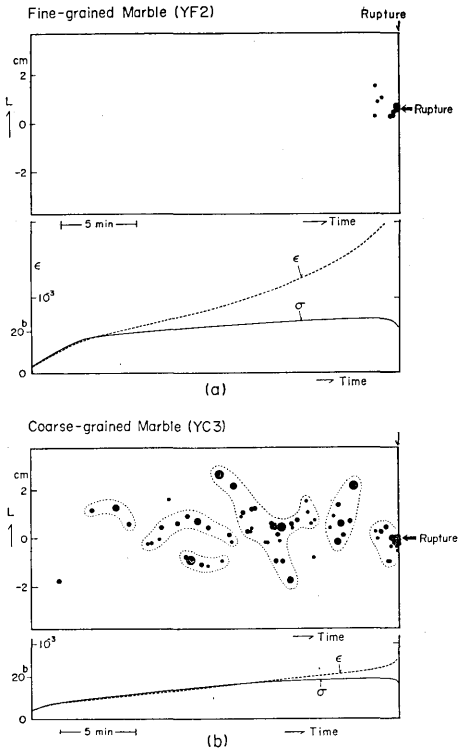

Fig. 6(a) and (b). Source locations of elastic shocks in the $\overline{OL}$ direction as functions of time in Yamaguchi marbles. (a): fine-grained marble; (b): coarse-grained marble. σ and ϵ: stress and strain at the tensile side of specimen.

grain sizes are about 0.2, 2, and 5 mm in diameter. The mechanical structure of fine-grained marbles is regarded as homogeneous in the investigated scale (e.g. Mogi, 1962a), and that of coarse-grained marbles is appreciably nonuniform. According to previous studies, fracturing behaviors are dependent on the structural heterogeneity, so that it is expected that the fracturing process systematically varies with grain sizes.

Figs. 6(a) and (b) show typical experimental results for the fine-grained marble (YF) and the coarse-grained marble (YC), respectively. Each upper figure indicates locations of sources of elastic shocks in the $\overline{OL}$

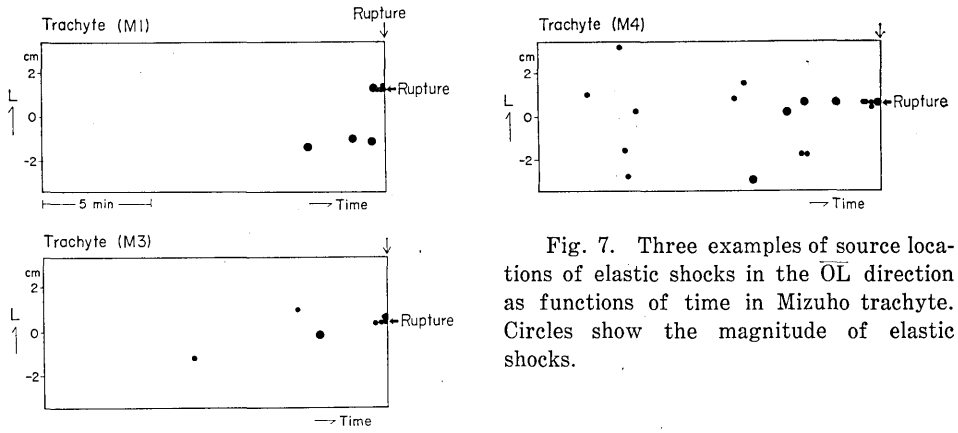

Fig. 7. Three examples of source locations of elastic shocks in the $\overline{OL}$ direction as functions of time in Mizuho trachyte. Circles show the magnitude of elastic shocks.

direction as functions of time. Different diameters of circles show different magnitudes of elastic shocks. Lower figures show the applied stress and the strain as functions of time. In the fine-grained marble with a homogeneous structure, any remarkable elastic shocks do not occur prior to a main rupture. In the coarse-grained marble, however, a number of elastic shocks continued to occur up to a main rupture. In this case, sources of elastic shocks do not locate at random, but with a tendency which seems to suggest the propagation of cracks. It is noteworthy that the occurrence of elastic shocks is not continuous up to the main rupture. Fracturing behaviors of the medium-grained marble were intermediate between the above-mentioned extreme cases. These results are consistent with the previous conclusion that the shock activity prior to the main rupture depends on the structural heterogeneity.

b) *Mizuho trachyte (a homogeneous silicate rock)*

As a nearly homogeneous silicate rock, the Mizuho trachyte with uniform structure, has been studied. Three examples of experimental results are represented in Fig. 7. A bending stress was applied very gradually before rupture, as in marbles. Only a few elastic shocks were observed before rupture, and the main rupture took place suddenly without any direct connection to preceding shocks. Observed elastic shocks are small in number, but they seem to be rather large in magnitude. However, the number of shocks was too few to discuss the magnitude-frequency relation of elastic shocks in this homogeneous rock.

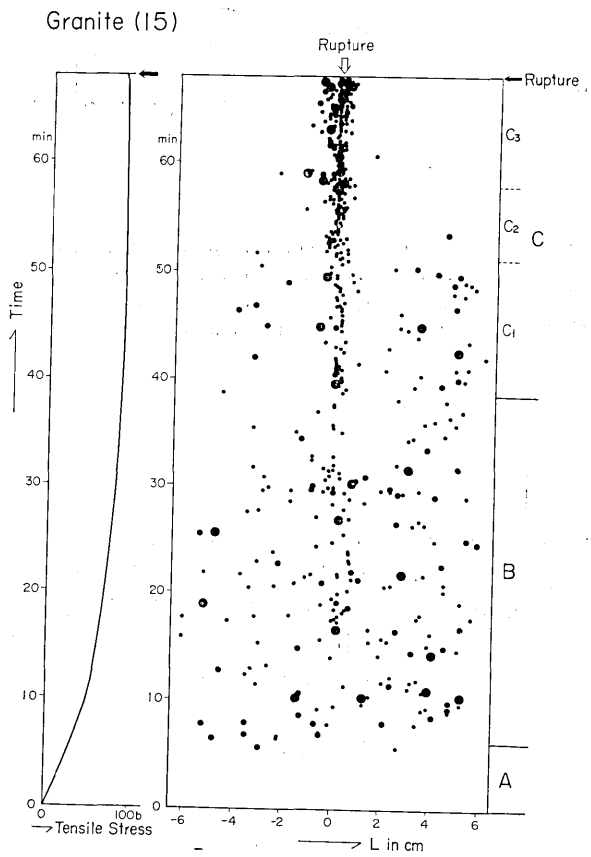

Fig. 8. Source locations of elastic shocks in the $\overline{OL}$ direction as functions of time in Inada granite (I5). **A**, **B** and **C** stages are indicated in the right side. Applied stresses (σ) at the tensile side are also shown as a function of time in the left figure.

c) *Granites (heterogeneous silicate rocks)*

As heterogeneous silicate rocks, Inada, Kitagi and Mannari granites have been studied in detail. In general, the process of occurrence of elastic shocks before rupture is devided into the following three stages; (**A**): Initial stage in which any appreciable elastic shocks do not occur. (**B**): In this stage, elastic shocks begin to occur and their sources locate randomly in the specimen. (**C**): The last stage in which sources of elastic shocks concentrate at limited regions. Some typical examples are explained below.

c-1) *A single fracture zone*

Fig. 8 shows a typical simple pattern of source locations. Elastic

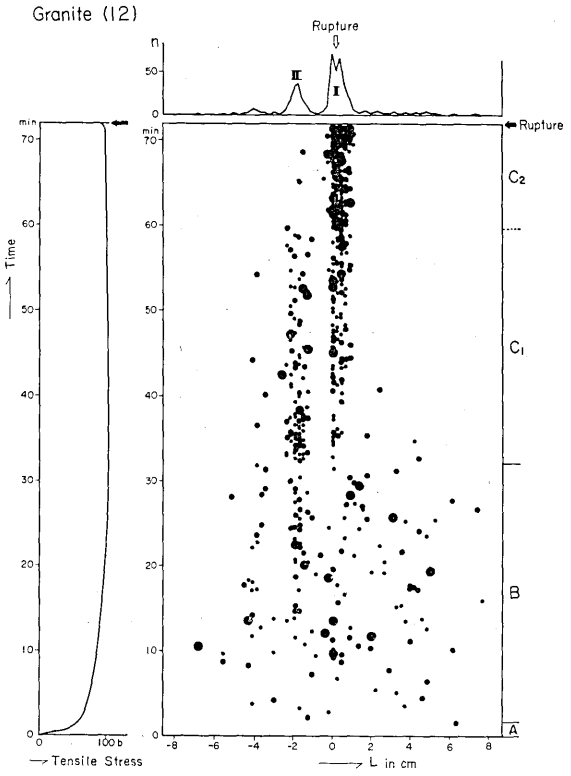

Fig. 9. Source locations of elastic shocks in the $\overline{OL}$ direction as functions of time in Inada granite (I2). A total distribution of sources is shown by a curve in the upper figure. Stresses at the tensile side are shown as a function of time in the left figure.

shocks begin to occur at a stress level and increase with the increase of the applied stress. In this stage (**B**), sources of elastic shocks locate at random in a direction of tensile stress. In the next stage (**C**), sources begin to concentrate at a region and they continue to occur at the region up to the main rupture. Activity in other regions decreases gradually with time, and just before rupture, source locations of elastic shocks are completely limited to the above-mentioned region where the main rupture will occur. The total frequency distribution of sources in the $\overline{OL}$ direction has a single sharp peak.

c-2) *Double fracture zones*

In this case, the total frequency distribution of sources in the $\overline{OL}$ direction has two peaks at **I** and **II** zones (Fig. 9). The micro-fracturing process is also divided into stages **A**, **B** and **C**. In stage **B**, sources of elastic shocks nearly randomly distribute, and at stage $\mathbf{C}_1$, they concen-

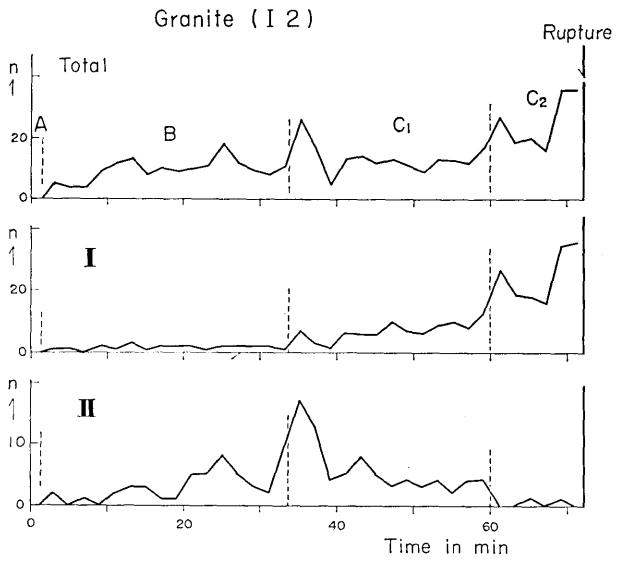

Fig. 10. Frequency curves of elastic shocks originated from the whole region (above), **I** zone (middle) and **II** zone (below). Stages **A**, **B** and **C** correspond to those in Fig. 9.

trate to **I** and **II** zones, and source locations at the last stage $\mathbf{C}_2$ are limited to **I** zone.

In Fig. 10, frequency curves of elastic shocks originated from **I** and **II** zones are represented together with the total frequency curve. The total frequency curve may suggest apparent stationary occurrence of elastic shocks except for the last stage ($\mathbf{C}_2$). However, the lower two curves indicate significant changes of the fracturing process. In stage **B**, the elastic shock activity markedly increased in **II** zone, but it was very low in **I** zone. At stage $\mathbf{C}_1$, the activity gradually decreased in **II** zone, but began to increase in **I** zone. At the last stage ($\mathbf{C}_2$), the activity completely decayed in **II** zone, but increased rapidly in **I** zone. The micro-fracturing activity in **I** zone was built up to the main rupture. Thus, adjacent zones closely interact on each other. This phenomenon will be discussed again in a later section.

c-3) *Triple fracture zones*

The pattern of source locations in Fig. 11 is more complex. The total frequency distribution of sources in $\overline{\mathrm{OL}}$ direction has three marked

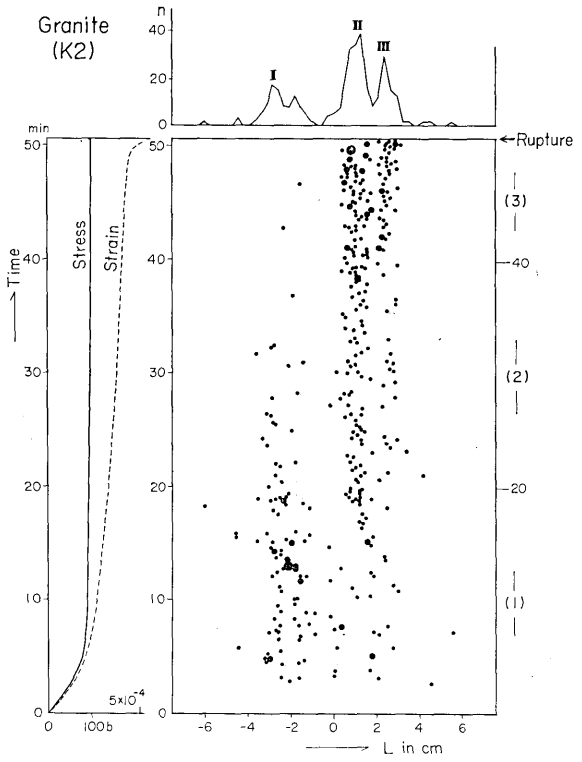

Fig. 11. Source locations of elastic shocks in the $\overline{OL}$ direction as functions of time in Kitagi granite (K2). A total distribution of sources is shown by a curve in the upper figure. Stress and strain at the tensile side are shown as functions of time in the left figure.

peaks at **I**, **II** and **III** zones. The source distributions in the stages (1), (2) and (3) are shown in Fig. 12. The most active region located at **I** zone in the initial stage (1), at **II** zone in the middle stage (2) and at **III** zone in the last stage (3). Thus, the active region systematically displaced with time in the $\overrightarrow{OL}$ direction. The observed macroscopic fracture pattern approximately agrees with locations of these active zones, as shown in Fig. 12.

In Fig. 13, the energies released by elastic shocks in **I**, **II** and **III** zones are shown as functions of time. The activity in **I** zone abruptly increased in the stage (1) and systematically decreased in the following stage. This curve is similar to a typical earthquake swarm curve. With decay of the activity in **I** zone, **III** zone became markedly active. The activity in **II** zone seems to show a pattern intermediate between the adjacent zones **I** and **III**.

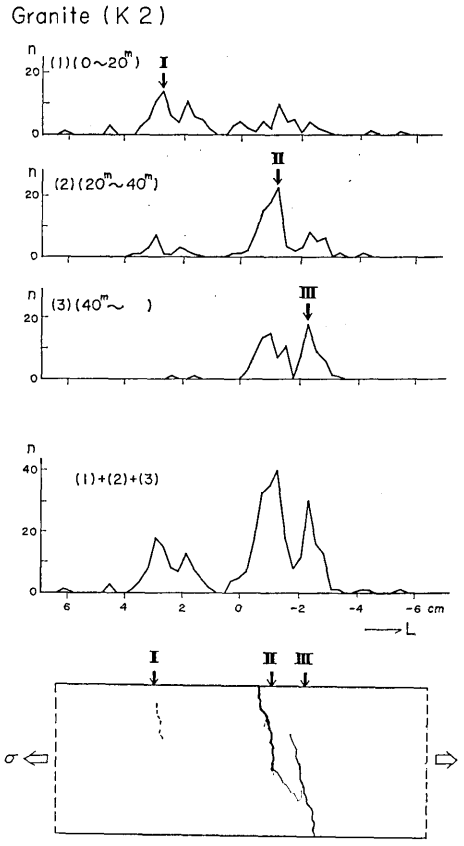

Fig. 12. Distributions of sonrces of elastic shocks in the $\overline{OL}$ direction in the (1), (2) and (3) stages, and their total distribution. A lower figure shows an observed main crack pattern.

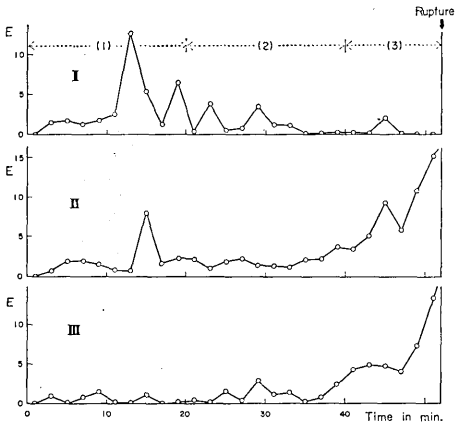

Fig. 13. Energies of elastic shocks originated from **I**, **II** and **III** zones as functions of time, in Kitagi granite (K2). The scale of energy is conventional.

3-2. Two-dimensional source locations of elastic shocks

The two-dimensional distributions of sources of elastic shocks have been studied for the above-mentioned various rock types. The results of heterogeneous silicate rocks, which are characterized by a high elastic shock activity, are very helpful to understand the fracturing process prior to rupture. Three examples are described below.

a) *Inada granite (I4)*

Fig. 14 shows the one-dimensional source locations as functions of time. This is a typical pattern of source locations in heterogeneous silicate rocks, as mentioned above. The two-dimensional source locations in successive stages are represented in Fig. 15. In stage **B**, sources distributed at random in the stressed region. At this stage, the location of the following main rupture cannot be predicted. In stage C_1, sources

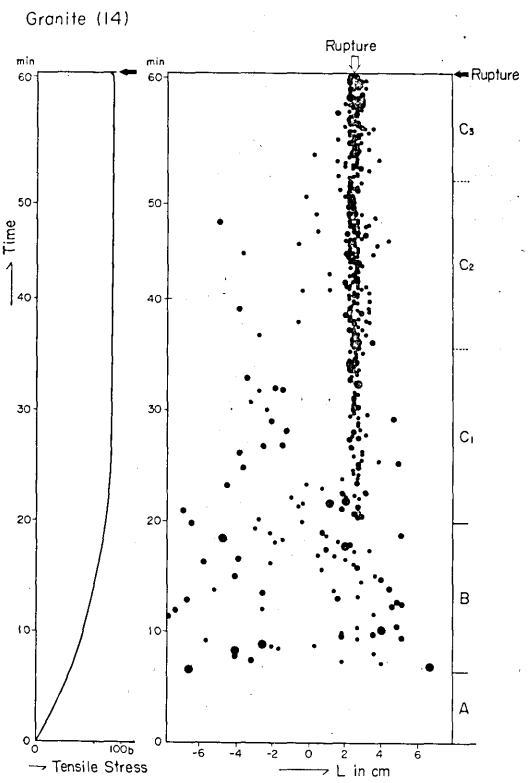

Fig. 14. Source locations of elastic shocks in the $\overline{OL}$ direction as functions of time in Inada granite (I4). Stresses at the tensile side are shown as a function of time in the left figure.

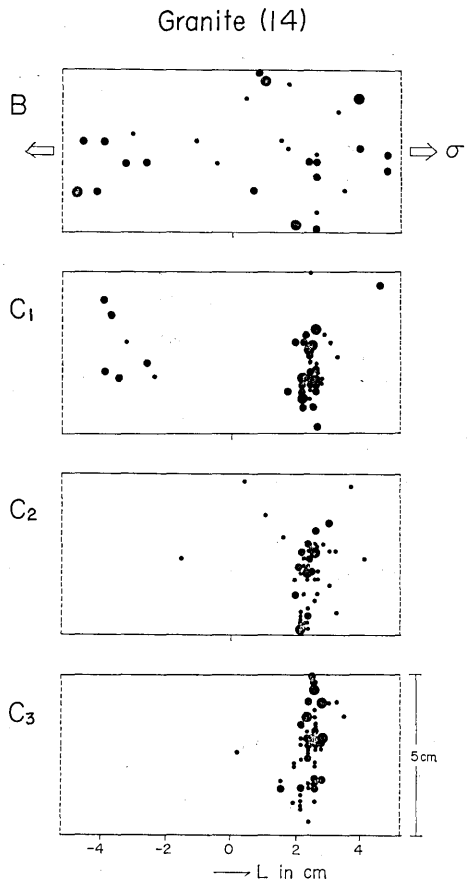

Fig. 15. Two-dimensional source locations of elastic shocks in successive stages in Inada granite (I4). Stages **B**, $\mathbf{C_1}$, $\mathbf{C_2}$ and $\mathbf{C_3}$ correspond to those in Fig. 14.

of elastic shocks began to occur concentratedly in a limited region. In stages $\mathbf{C_2}$ and $\mathbf{C_3}$, the source region developed in the direction perpendicular to the applied tensile stress up to the main rupture.

The successive development of the active area before the main rupture is represented with the main crack pattern in Fig. 16. The highly active areas, the shaded areas in this figure, successively migrated outward, and an area where the activity had been markedly high in a preceding stage became relatively calm in the following stage. This

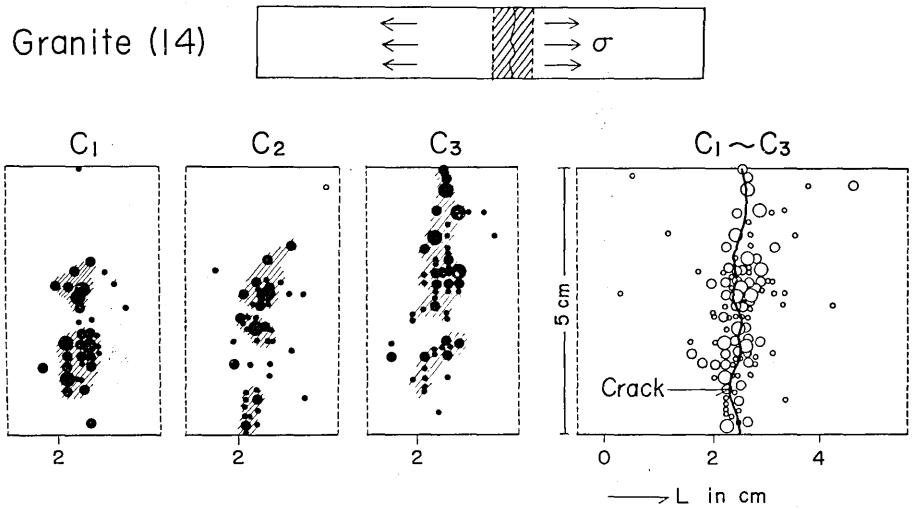

Fig. 16. Successive development of the source region of elastic shocks in the stages C_1～C_3 and an observed main crack pattern.

feature in the fracturing process is seen in the seismic activity in fields, as will be mentioned in a later section. In Fig. 16, the main fracture pattern observed after the experiment is compared with the source locations of elastic shocks. This result suggests that the above-mentioned development of the source region indicates the successive propagation of rupture.

b) *Inada granite (I5)*

The one-dimensional source locations in this case was described in c-1) in the preceding section (Fig. 8). The areal distributions of sources in successive stages are shown in Fig. 17. In stage **B**, the activity of elastic shocks was markedly high and source locations were also at random and any linear locations suggesting the future development of fracturing could not be found. In the next stage (C_1), some weak concentration of sources took place at the center of the investigated area. The concentration of sources in the limited area became evident in the following stage C_2, and the source area developed to the whole width of the sample in the last stage C_3. In Fig. 18, the successive development of the source area in stages C_2 and C_3 is shown with the main fracture pattern observed after the experiment. The curved shape

of the source region in stage C_3 corresponds well to the observed fracture pattern.

c) *Shirochōba andesite (S2)*

The one- and two-dimensional source locations in this case are shown in Figs. 19 and 20. The process is also devided into three stages **A**, **B** and **C**, but the elastic shock activity is noticeably lower in andesites than in granites. The concentration of sources of elastic shocks to a linear zone perpendicular to the direction of the tensile stress was also found, but the degree of concentration of sources to a narrow zone seems to be somewhat lower than that in granites. A regular distribution of sources along a line was observed in stage C_2. Further study of fine patterns of source locations may clarify the fracturing process in more detail.

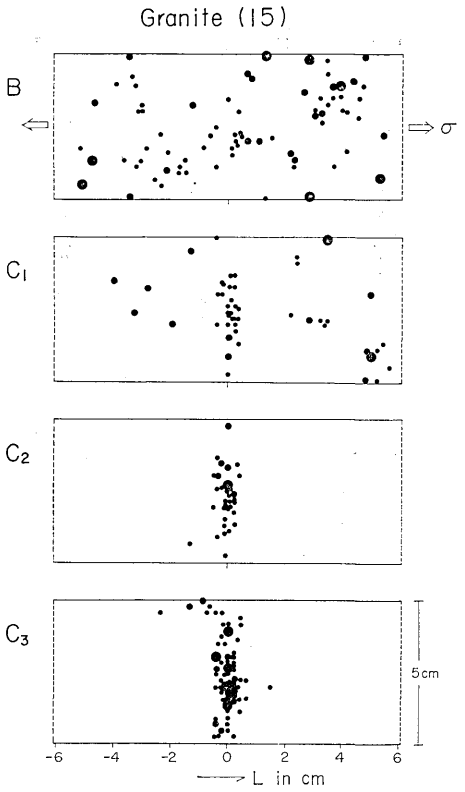

Fig. 17. Two-dimensional sources locations of elastic shocks in successive stages in Inada granite (I5). Stages **B**, C_1, C_2 and C_3 correspond to those in Fig. 8.

4. Discussion

4-1. Micro-fracturing process prior to rock failure

The previous papers (e.g. Mogi, 1962a) showed that studies of elastic shocks caused by micro-fracturing provide fundamental information on the mechanism of rock failure. In these previous studies, however, the number and the energy of elastic shocks originating from the whole sample, without any consideration of source locations, have been discussed. In the present study, the source locations of elastic shocks in successive stages of fracturing have been obtained.

With consideration of source locations of elastic shocks, the micro-

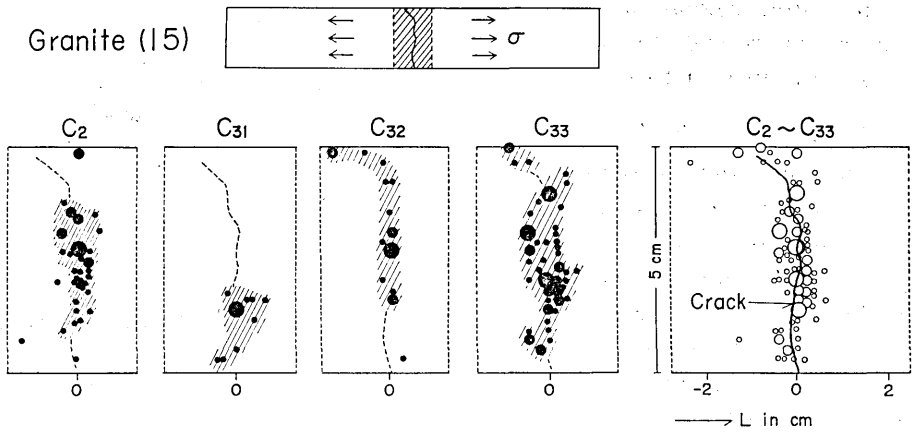

Fig. 18. Successive development of the source region of elastic shocks in the stages C_2 and C_3 and an observed main crack pattern.

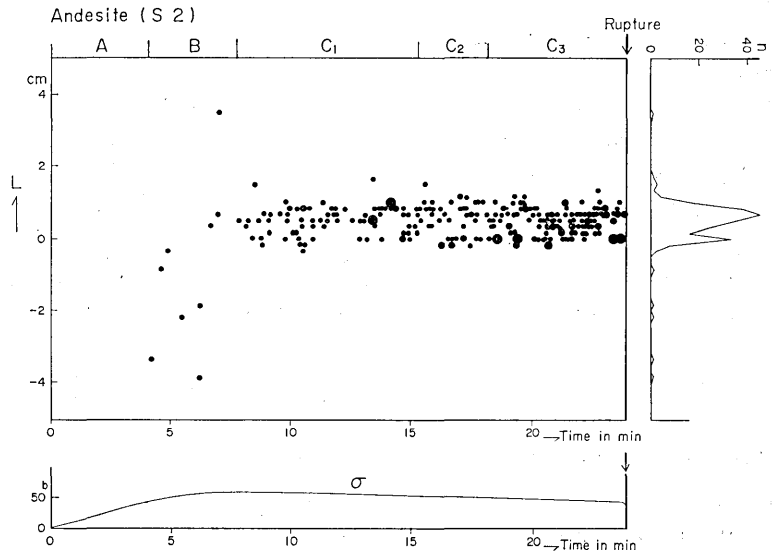

Fig. 19. Source locations of elastic shocks in the $\overline{OL}$ direction as functions of time in Shirochōba andesite (S2). A total distribution of sources is shown by a curve in the right side. σ: stress at the tensile side.

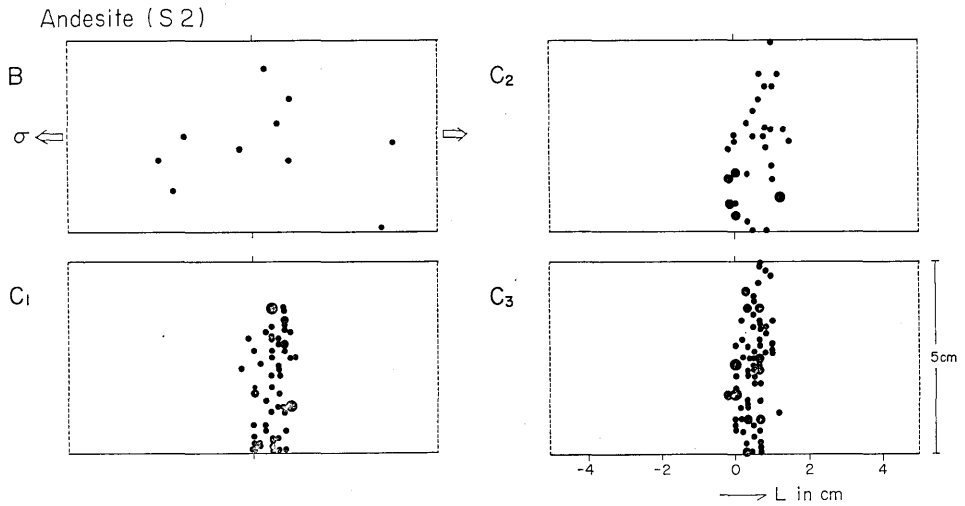

Fig. 20. Two-dimensional source locations of elastic shocks in successive stages in Shirochōba andesite (S2). Stages **B**, $\mathbf{C}_1$, $\mathbf{C}_2$ and $\mathbf{C}_3$ correspond to those in Fig. 19.

fracturing process of rocks subjected to an increasing stress is devided into three stages **A**, **B** and **C**. In stage **A**, any elastic shock activity is not observed, because the stress level is too low to cause micro-fracturing. In the next stage (**B**), elastic shocks occur randomly in the specimen, without appreciable concentration of their source locations. In stage **C**, many sources concentrate in one or more limited regions, and the activity in other regions decreases. Micro-fractures in one of the active regions develope to the main rupture.

These three stages are all observed in heterogeneous rocks, such as granites, but stages **B** and **C** are not observed in rocks with uniform structures, such as fine-grained marbles and Mizuho trachyte.

In most cases, the main crack was a tensile one perpendicular to the direction of the applied tension. All micro-cracks are also tensile ones perpendicular to the applied tension, because initial motions of P-waves of elastic shocks are clearly directed outward at P_1 and P_2 which are situated in the direction of the applied tension. Thus, the observed successive development of the source region just before rupture suggests the process that the main rupture takes place by developoment of a densely cracked region in that direction.

In stage **C**, interaction between adjacent fracturing regions was

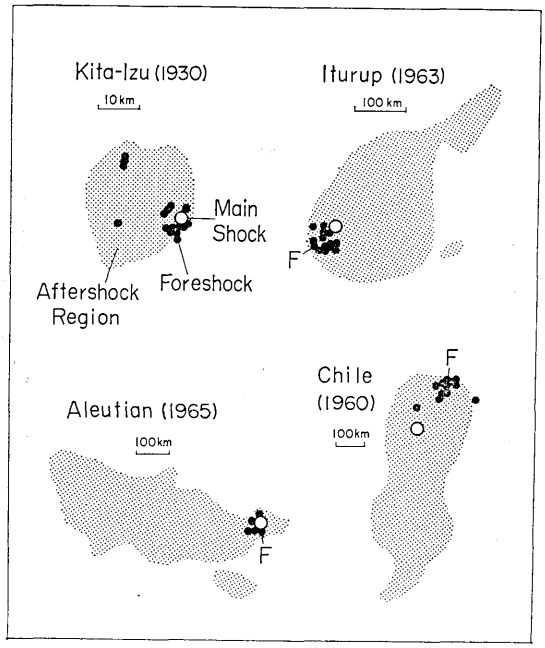

Fig. 21. Epicentral distributions of foreshocks, a main shock, and an aftershock region, in Kita-Izu earthquake (1930), Iturup earthquake (1963), Aleutian earthquake (1965) and Chilean earthquake (1960).

sometimes observed, as mentioned above. This process is shown typically in Fig. 10. The activity in I zone begins to increase with the decrease of the activity in the adjacent zone II where the micro-fracturing activity was high in the preceding stage. This process may be understood as follows. The micro-fracturing activity in II zone under increasing stress decreased by the stop of crack propagation caused by some barriers, so that higher stresses were needed for further propagation of cracks in II zone. In this stage, another crack I which was stronger than II at the preceding stage began to propagate. Such compensative occurrence of elastic shocks in adjacent regions is very interesting, because a similar feature is seen in earthquake occurrence.

4-2. Relation to earthquake phenomena

(i) The observed micro-fracturing process prior to rupture is very suggestive of the foreshock phenomena in earthquakes. In non-uniform structures, the foreshock activity prior to a main shock may increase

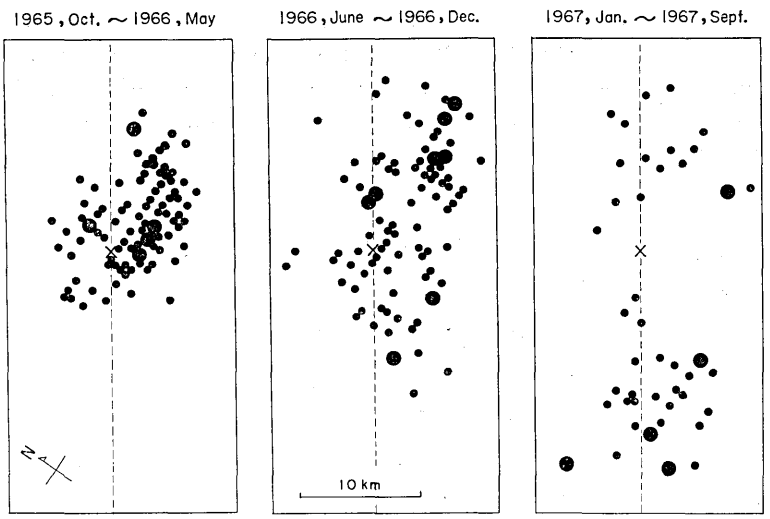

Fig. 22. Epicentral distributions of earthquake ($M \geq 4.0$) during three successive periods in Matsushiro earthquake swarm (Data from the Seismological Bulletin of Japan Meteorological Agency).

with the following processes: with the increase of stress, the foreshock activity gradually increases in a wide area (stage **B**) and then sources of foreshocks concentrate in a limited region near the epicenter of the main shock (stage **C**). Such concentrative occurrence of foreshocks just before the main shock was found in several cases for which foreshock locations are known. Fig. 21 shows examples of epicentral locations of foreshocks, a main shock, and aftershocks (Mogi, 1967a). However, the above-mentioned foreshock phenomenon cannot be expected in homogeneous structures.

In relation to earthquake prediction problems, it is very important to note how foreshocks just before a main shock are discriminated from other shocks. Further detailed study of elastic shocks may provide some clue to solving this problem.

(ii) The migration feature of fracturing activity, shown in Fig. 16, is also found in earthquakes. In the recent Matsushiro earthquake swarm, marked expansion of source region has been observed (Hagiwara, 1967). Fig. 22 shows epicentral distributions of larger shocks ($M \geq 4.0$) in three successive periods. The highly active region migrated into the southwest and the north-east directions. The region which was active in the

initial period became calm in the following stages, and the active regions migrated outward in the NE-SW direction. This feature is very similar to that in source regions of elastic shocks, which is shown in Fig. 16, and so this feature may be explained as the fundamental one in fracture propagation.

Aknowledgement

The author wishes to thank Mr. Kansaku Igarashi and Miss. Sagako Takahashi for their assistance in the experiment.

References

HAGIWARA, T., 1967, Geodetic and geophysical investigations of Matsushiro earthquake swarm, in *Seismology in Japan, Zisin*, [II], **20**, No. 4, 192-200.

MOGI, K., 1962a, Study of elastic shocks caused by the fracture of heterogeneous materials and its relations to earthquake phenomena, *Bull. Earthq. Res. Inst.*, **40**, 125-173.

MOGI, K., 1962b, The fracture of a semi-infinite body caused by an inner stress origin and its relation to earthquake phenomena, 1, *Bull. Earthq. Res. Inst.*, **40**, 815-829.

MOGI, K., 1962c, Magnitude-frequency relation for elastic shocks accompanying fractures of various materials and some related problems in earthquakes, 2, *Bull. Earthq. Res. Inst.*, **40**, 831-853.

MOGI, K., 1963a, The fracture of a semi-infinite body caused by an inner stress origin and its relation to earthquake phenomena, 2, *Bull. Earthq. Res. Inst.*, **41**, 595-614.

MOGI, K., 1963b, Some discussions on aftershocks, foreshocks and earthquake swarms—the fracture of a semi-infinite body caused by an inner stress origin and its relation to earthquake phenomena, 3, *Bull. Earthq. Res. Inst.*, **41**, 615-658.

MOGI, K., 1964, Deformation and fracture of rocks under confining pressure (1) Compression tests on dry rock sample, *Bull. Earthq. Res. Inst.*, **42**, 491-514.

MOGI, K., 1965, Deformation and fracture of rocks under confining pressure (2) Elasticity and plasticity of some rocks, *Bull. Earthq. Res. Inst.*, **43**, 349-379.

MOGI, K., 1966, Pressure dependence of rock strength and transition from brittle fracture to ductile flow, *Bull. Earthq. Res. Inst.*, **44**, 215-232.

MOGI, K., 1967a, On foreshocks and earthquake swarms, in *Seismology in Japan, Zisin*, [II], **20**, No. 4, 143-146.

MOGI, K., 1967b, Earthquakes and fractures, *Tectonophysics*, **5**, 35-55.

NAGUMO, S., and K. HOSHINO, 1967, Occurrence of micro-fracturing shocks during rock deformation with a special reference to activity of earthquake swarms, *Bull. Earthq. Res. Inst.*, **45**, 1295-1311.

OBERT, L., and W. DUVALL, 1945, The microseismic method of predicting rock failure in underground mining, 2. Laboratory experiments, *U.S. Bur. Mines Rept. Invest.*, **3803**, 1-14.

SCHOLZ, C. H., 1968a, Microfracturing and the inelastic deformation of rock in compression, *J. Geophys. Res.*, **73**, 1417-1432.

SCHOLZ, C. H., 1968b, Experimental study of the fracturing process in brittle rock, *J.*

Geophys. Res., **73**, 1447-1454.

SUZUKI, Z., and HAMAGUCHI, 1966, The brittle fracture of tempered glass and its relation to the occurrence of earthquakes (1), *Sci. Rept. Tôhoku Univ.*, 5, **5**, 177-182.

VINOGRADOV, S. D., 1962, Experimental study of the distribution of the number of fractures in respect to the energy liberated by the destruction of rocks, *Bull. Acad. Sci. U.S.S.R., Geophys. Ser.*, (eng. ed.), 1292-1293.

WATANABE, H., 1963, On the sequence of earthquakes, *Spec. Contr., Geophys. Inst., Kyôto Univ.*, **4**, 153-192.

---

53. 岩石の破壊過程における Elastic Shocks の震源分布 (1)

地震研究所　茂　木　清　夫

不均質な岩石に力を加えてゆくと，局部的な破壊に伴う衝撃性弾性波 (Elastic Shocks) が発生し，それが次第に増加して主破壊に至るが，その発生過程は岩石の構造と密接な関係を示すことは すでに報告した所である．これまでは，この過程を研究するのに，主として，Elastic Shocks の頻度やエネルギーの変化に注目したが，更に，波動特性や震源分布の特徴を明らかにすることが重要である．本論文では，この様な目的のため今回開発した測定法について述べ，それを用いて震源分布を求めた結果を述べた．今回は各種岩石の常圧下の曲げ試験を行なったが，その場合の岩石の主破壊に至る過程は，Elastic Shocks の震源分布を考慮して，次の様に要約される．

(1) 主破壊に至る過程は次の三段階に分けられる．

A: Elastic Shocks が未だ発生しない低応力段階．

B: Elastic Shocks が起こるが，その震源は試料内に一様に分布する段階．

C: Elastic Shocks の震源が限られた所に集中する段階で，最後にその集中箇所の一つで主破壊が発生する．

(2) 不均一構造をもつ岩石 (例えば花崗岩) では，上記の三つの段階が明瞭に認められるが，構造均一な岩石 (例えば山口産微晶質大理石) では，**B** や **C** の段階が明瞭ではなく，主破壊が突然発生する．

更に主破壊に先行して発生する Elastic Shocks の起こり方と，大きい地震の前震のそれとの類似性について考察した．
